Dynamic heterogeneities, boson peak, and activation volume in glass-forming liquids

L. Hong,[1] V. N. Novikov,[2,3,4,*] and A. P. Sokolov[2,3]

[1]*Center for Molecular Biophysics, Oak Ridge National Laboratory, Oak Ridge, Tennessee 37831, USA*

[2]*Department of Chemistry, University of Tennessee, 1420 Circle Drive, Knoxville, Tennessee 37996, USA*

[3]*Chemical Sciences Division, Oak Ridge National Laboratory, Oak Ridge, Tennessee 37831, USA*

[4]*IA&E, Russian Academy of Sciences, Novosibirsk, 630090, Russia*

(Received 3 March 2011; revised manuscript received 12 May 2011; published 30 June 2011)

There are various arguments and models connecting the characteristic length associated with the boson peak vibrations ξ to the length scale of dynamical heterogeneity $L_{\rm het}$. ξ is usually defined as the ratio of the transverse sound velocity to the boson peak frequency. Here we present pressure, temperature, and molecular weight dependencies of ξ, estimated using light scattering, in a few molecular and polymeric glass formers. These dependencies are compared with respective dependencies of the activation volume $\Delta V^{\#}$ in the same materials. Good agreement is found for the pressure and molecular weight dependencies of ξ and $\Delta V^{\#}$ measured at the glass transition temperature T_g. These results provide more evidence for a possible relationship between the sensitivity of structural relaxation to density (activation volume) and the heterogeneity volume. However, contrary to the expectations for $L_{\rm het}$, ξ does not decrease with temperature above T_g in most of the studied materials. The temperature dependence of ξ is compared to that of $L_{\rm het}$ in glycerol and orthoterphenyl (OTP) estimated from literature data. The analysis shows a clear difference in the behavior of $\xi(T)$ and $\Delta V^{\#}(T)$ at temperatures above T_g, although $\Delta V^{\#}(T)^{1/3}$ and $L_{\rm het}(T)$ have similar temperature dependence. Possible reasons for the observed difference are discussed.

DOI: 10.1103/PhysRevE.83.061508 PACS number(s): 64.70.P−, 78.35.+c

I. INTRODUCTION

Although dynamic heterogeneities in supercooled liquids have been known for a long time (see reviews [1–4] and references therein), interest in their study has grown rapidly during the recent decade [5–21]. The interest appears to be in all kinds of studies—theoretical, computational, and experimental. It is related not only to the description of stretched relaxation spectra and of the decoupling in dynamics (e.g., decoupling of diffusion and rotation [1], chain and segmental dynamics [22]), but the deep fundamental understanding of the glass transition phenomena. Existence of dynamic heterogeneities on a time scale comparable to the structural relaxation τ_α has been visualized in computer simulations [3,4] and in optical microscopy studies of colloidal systems [4,6]. From an experimental point of view, it is difficult to provide direct measurement of the heterogeneity length scale $L_{\rm het}$. The usual linear susceptibilities and scattering intensities (two-point correlation functions) do not give information on the length of dynamical heterogeneity. It has been demonstrated that only higher-order (e.g., three-point, four-point, etc.) correlation functions might provide the required information [7–9,11, 14,17–20,23]. One of the most direct experimental methods for measurements of $L_{\rm het}$ is based on four-dimensional (4-D) NMR [15,16]. It has been applied to four glass-forming systems (glycerol, orthoterphenyl (OTP), poly(vinyl acetate) (PVAc), and sorbitol) and $L_{\rm het}$ was estimated to be ∼1.5–3.5 nm [16]. However, due to the complexity of the method, the accuracy of these estimates of $L_{\rm het}$ was not sufficient for systematic studies of, e.g., temperature variations of $L_{\rm het}$ [24].

Recently, the authors of Refs. [17,25] proposed a method to estimate the dynamic heterogeneity. It is based on a derivative analysis of the two-point correlation function that provides the parameter χ_T. The latter is the lower limit for the four-point correlation function $\chi_4(t)$ that directly measures dynamic heterogeneity [17]. This approach seems to be rather simple and attractive and has been applied to many materials [17]. However, the obtained results cast some doubt on the validity of this analysis:

(i) The reported increase in the number of particles involved in heterogeneities with temperature decrease is too high (∼100 times). The usual expectation is that this number should change by a factor of ∼2–10.

(ii) The increase is weak at temperatures approaching the glass transition T_g and happens mostly at higher temperature.

(iii) Moreover, the strongest change in χ_T appears at high temperatures, where structural relaxation exhibits Arrhenius temperature variations. This is especially suspicious because no model expects variations in the scale of dynamic heterogeneity at this temperature range.

Based on this analysis, we will not use the results of this approach in our discussion. Another very recent publication used the nonlinear dielectric response χ_3 for estimates of temperature variations of the number of dynamically correlated structural units $N_{\rm het}$ [20]. The theoretical basis for this approach was formulated in [18] and the first experimental studies were performed on glycerol [20]. Although the method does not provide absolute values for $N_{\rm het}$, it allows study of its temperature variations with reasonable accuracy.

The dynamical heterogeneities appear not only in the structural relaxation, but also in the fast picosecond dynamics [5,26] and persist also in the glassy state [21]. In these cases dynamic heterogeneity appears, e.g., in the mean-squared displacements of structural units $\langle u^2 \rangle$, and is determined by

*novikov@utk.edu

short-time dynamics [5,27,28], basically by vibrations. The heterogeneity of $\langle u^2 \rangle$ in the first approximation is associated with the spatial fluctuations of local elastic constants [27]. The latter are assumed to be frozen in the glassy state. It is known that the spatial fluctuations of elastic constants with a correlation radius ξ produce an excess density of vibrational states, i.e., the boson peak, at a frequency $\nu_{\rm bp}$ connected to ξ by the equation

$$\xi = Sc_t/\nu_{\rm bp}, \tag{1}$$

where c_t is the transversal sound velocity and S is a constant of the order of 1 [28–30]. The boson peak is general for all glass-forming materials and presents an excess (relative to the expected in the Debye model) density of vibrational states at frequencies around ~1 THz [31,32]. It is usually analyzed as the peak in density of states $g(\nu)$ divided by ν^2. $g(\nu)/\nu^2$ should be a constant in the Debye model, but has the maximum (the boson peak) in glasses. Although detailed theoretical description of the boson peak is not developed yet, the connection of the boson peak to fluctuations of elastic constants has been demonstrated in Ref. [33]. Still, we want to emphasize that the connection of the boson peak to heterogeneity length scale [Eq. (1)] is an assumption and there are different interpretations of the excess density of the vibrational states. Moreover, the relationship between ξ and $L_{\rm het}$ is unclear.

In Refs. [5,26] it was shown from simulations that the short-time dynamical heterogeneities correlate with the heterogeneities in the structural relaxation: The particles that have large diffusion displacements on time scales of τ_α are the particles that have large mean-squared displacements due to the fast dynamics. It means that the length scale associated with the boson peak (fast dynamics) might reflect the size of dynamical heterogeneity in structural relaxation. This idea was also proposed in several theoretical works, including random first order transition theory (RFOT) [34] and a paper by de Gennes [35]. Indeed, the direct comparison presented in Refs. [36,37] shows that ξ estimated from the boson peak at T_g has the same value as $L_{\rm het}$ for structural relaxation in all four materials studied by 4-D NMR. So, there is computational, theoretical and experimental evidence suggesting that the length scale estimated from the boson peak ξ might reflect the size of dynamic heterogeneities of structural relaxation $L_{\rm het}$. Many more experimental data are available for the boson peak than for the dynamical heterogeneity of the structural relaxation. This might open the way to analyze the scale of dynamic heterogeneities in many materials. In this paper we check the hypothesis about the relation between the boson peak and dynamical heterogeneities by comparing their material, pressure, and temperature dependence.

In our recent studies we used this approach to analyze the relationship between ξ at T_g and the fragility of glass-forming materials m [36,37]. The latter is defined as

$$m = \left. \frac{d\lg\tau_\alpha}{dT_g/T} \right|_{T=T_g}, \tag{2}$$

and characterizes the deviation of the temperature dependence of τ_α from the Arrhenius behavior. It has been found that $\xi(T_g)$ does not correlate with fragility, in agreement with other data [16,25] and in contradiction with traditional expectations. The analysis, however, reveals that $\xi(T_g)$ correlates well with one part of fragility—the volume (density) dependence of the structural relaxation. The latter is usually characterized by the activation volume $\Delta V^\#$, defined through the pressure dependence of τ_α at constant T [38]:

$$\tau_\alpha(T,P) = \tau_\alpha(T,0)\ \exp(P\Delta V^\#/kT), \tag{3}$$

where P is pressure. It was shown that $\xi(T_g)$ correlates with $\Delta V^\#(T_g)$ in different glass-forming materials—molecular, covalent, and polymeric systems [36,37]. Moreover, it appears that $\Delta V^\#$ in all these materials is a fraction (~3%–5%) of the heterogeneity volume defined as ξ^3.

The main goal of the present paper is to further verify the proposed relationship between the heterogeneity length scale estimated from the boson peak and the activation volume. We analyzed the influence of molecular weight (MW) in polymers on both parameters, with special focus on poly(propylene glycol) (PPG), where an increase in MW leads to change of the material from predominantly hydrogen bonding to a van der Waals system [38]. We also analyzed the influence of pressure on both parameters in several glass-forming systems. All these measurements confirmed the discovered earlier correlations between $\xi(T_g)$ and $\Delta V^\#(T_g)$. However, analysis of the temperature dependence of $\xi(T)$ above T_g performed for several materials did not reveal any significant changes. This disagrees with the well-known decrease of $\Delta V^\#(T)$ with temperature above T_g [39–42]. For the example of glycerol we demonstrate that $\Delta V^\#(T)$ seems to follow $N_{\rm het}(T)$ estimated from nonlinear dielectric studies. Possible explanations for the difference in behavior of $\xi(T)$ and $\Delta V^\#(T)$ are discussed at the end.

II. EXPERIMENTAL

Most of the materials used in our studies were purchased from commercial sources: Glycerol, salol, orthoterphenyl (OTP), cumene, sorbitol, propylene glycol (PG), di(propylene glycol) (DPG), tri(propylene glycol) (TPG), and poly(propylene glycol) (PPG) with M_w=4000 g/mol, M_n = 3500 g/mol are from Sigma-Aldrich (M_w and M_n are weight average and number average molecular weights). Polyisoprene (PIP) with M_w = 2450 g/mol, M_n = 2410 g/mol, poly(vinyl acetate) (PVAc) with M_w = 184,100 g/mol, M_n = 61,600 g/mol, polycarbonate (PC) with approximate M_w = 60,000 g/mol and polystyrene (PS) with M_w = 580 g/mol, M_n = 540 g/mol are from Scientific Polymer. Poly(methyl phenyl siloxane) (PMPS) with M_w = 25,600 g/mol, M_n = 15,800 g/mol and PS with M_w = 223,000 g/mol, M_n = 200,600 g/mol are from Polymer Source. Polyisobutylene (PIB) with M_n = 20,000 g/mol was synthesized at Akron University (Akron, OH). The samples were placed in a homemade optical cell with two parallel sapphire windows, and then the cell was mounted into the optical cryofurnace to be cooled down to a desired temperature.

The depolarized light scattering spectra were measured at 90° in a symmetric geometry [43]. This geometry compensates for the refractive index and provides an estimate of sound velocities from the Brillouin scattering spectra without knowledge of the refractive index [44]. We used a solid-state

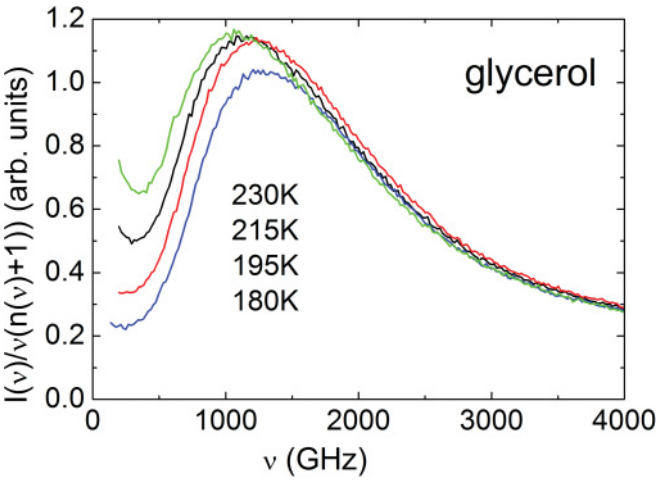

FIG. 1. (Color online) Light scattering spectrum of the boson peak in glycerol at $T = 230$, 215, 195, and 180 K, from top to bottom.

laser (Verdi-2 from Coherent) with a wavelength of 532 nm and power ∼50–150 mW on the sample. Brillouin spectra were measured using a tandem Fabry-Perot interferometer (Sandercock model). The low frequency Raman spectra were measured using a Jobin Yvon T64000 triple monochromator. A commercial anvil pressure cell from D'Anvils was used for hydrostatic pressure up to 1.5 GPa. For measurement of the applied pressure we used the ruby fluorescence method, which is a well established technique [45]. Details of the pressure measurements can be found in [43].

For the temperature studies of ξ, we focus on a temperature range mostly above T_g, because the structure of the materials is frozen in the glassy state, and ξ does not exhibit any measurable temperature dependence. Here we chose three materials, PIB, OTP, and glycerol, as representatives to perform this study. The investigated temperature range for glycerol is from 180 to 235 K ($0.95T_g$–$1.25T_g$), for OTP from 230 to 265 K ($0.95T_g$–$1.1T_g$), and for PIB from 180 to 260 K ($0.95T_g$–$1.3T_g$). In the case of glycerol, the transverse sound waves above 235 K are not measurable by Brillouin spectroscopy, whereas for OTP and PIB, the boson peak overlaps strongly with the quasielastic scattering above 265 K. The latter makes estimates of the boson peak strongly model dependent. Details of the spectra analysis, estimates of the boson peak frequency, and of the transverse sound velocity are described in our earlier paper [36].

As an example, Fig. 1 presents the boson peak spectra in glycerol at different temperatures. The temperature dependence of the boson peak frequency and the transversal Brillouin line frequency in glycerol are shown in Fig. 2. Similar results have been obtained also for OTP and PIB (are not shown) and will be discussed in Sec. III C.

III. RESULTS AND DISCUSSION

A. Polymers with different molecular weight

We start our discussion from the analysis of $\xi(T_g)$ in polymers with various molecular weights. It is well known that change in the molecular weight of polymers leads to change in their fragility and fast dynamics [46,47]. In particular, fragility increases with MW in PS [46] (this seems to be a general trend for polymers [32]) while it slightly decreases in PIB [47]. Figure 3 presents the dependence of $\xi(T_g)$ on the degree of polymerization (number of monomers). $\xi(T_g)$ increases with MW in PS and PPG, while it slightly decreases in PIB. The opposite behavior of PS and PIB correlates with the MW dependence of fragility in these polymers, as has already been emphasized in [36]. Presenting $\xi(T_g)$ for these polymers as a function of their fragility (Fig. 4) clearly indicates that there is no correlation between these two parameters, although there is a clear trend. PPG has a fragility similar to PIB and low molecular weight PS, but $\xi(T_g)$ is clearly smaller.

Let us focus on the behavior of PPG. This material presents particular interest because its monomer is a traditional hydrogen-bonding system. However, increase in MW leads to strong diminishing of the role of H bonds which are only at the end of the chains. Thus increase in the chain length leads to a transition from the H-bonding system to the van der Waals system in the case of PPG. This transition reflects, in particular, MW dependence of fragility in PPG [48]. It is known that temperature dependence of relaxation time τ_α has two contributions, one pure thermal (at constant volume) and another one due to change in volume (density) [38]. The same is applicable to fragility that can be presented as

$$\begin{aligned} m &= \left(\frac{\partial \lg \tau_\alpha}{\partial \frac{T_g}{T}}\right)_P\Bigg|_{T=T_g} = \left(\frac{\partial \lg \tau_\alpha}{\partial \frac{T_g}{T}}\right)_V\Bigg|_{T=T_g} \\ &\quad + \left(\frac{\partial \lg \tau_\alpha}{\partial P}\right)_T\Bigg|_{T=T_g} \left(\frac{\partial P}{\partial \frac{T_g}{T}}\right)_V\Bigg|_{T=T_g}, \\ &= m_V + \frac{\Delta V^\#}{k_B \ln 10}\,\frac{\alpha_T}{\kappa}. \end{aligned} \tag{4}$$

Here m_V is the isochoric fragility (pure thermal contribution), κ is compressibility, and α_T is the thermal expansion coefficient of the supercooled liquid at T_g. The second term on the right-hand side presents the volume contribution to fragility, m–m_V. Similar to most of the hydrogen-bonding systems, m_V dominates the total fragility in propylene glycol (monomer). However, m–m_V increases sharply with MW in PPG, while isochoric fragility remains essentially unchanged [49] (Fig. 5). As a result, the volume contribution to fragility in long PPG chains becomes comparable to m_V, the behavior characteristic for most of the van der Waals systems. Thus PPG presents a unique system for testing the relationship between the length scale of heterogeneity and the volume contribution to fragility. As has been shown in Ref. [36], α_T/κ at T_g does not vary much between different systems and one can write m–$m_V \propto \Delta V^\#$. If the proposed relationship is correct, then one expects m–$m_V \propto \xi^3$. Indeed variations of the heterogeneity volume ξ^3 with MW in PPG correlate well with the variations of the volume contribution to fragility (Fig. 5).

Figure 6 presents a double-logarithmic plot of ξ vs $\Delta V^\#$ for PS and PPG with different molecular weights. Unfortunately, we did not find literature data to estimate $\Delta V^\#$ for PIB with different molecular weight. The linear fit of the data for PS and PPG (Fig. 6) again reveals the proportionality between ξ^3 and $\Delta V^\#$, in agreement with our earlier studies for different

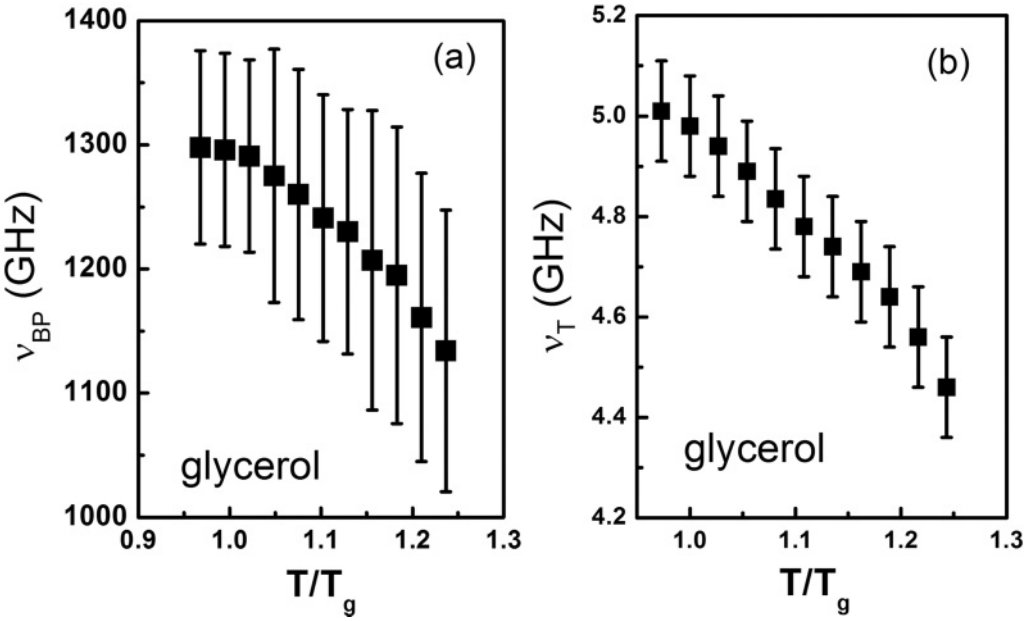

FIG. 2. Temperature dependence of the boson peak frequency (a) and the transversal Brillouin mode frequency (b) in glycerol.

systems. This analysis provides more experimental evidence for the correlation between the dynamic heterogeneity volume and activation volume discovered in Ref. [36].

B. Influence of pressure

According to Eq. (1) the length scale associated with the boson peak is determined by the ratio of the transverse sound velocity to the frequency of the boson peak. It is known that both these parameters increase with pressure. Recently we measured the longitudinal and transverse sound velocities as well as the boson peak frequency under pressure in a series of molecular and polymeric materials [43]. These data provide information on the behavior of the heterogeneity length scale ξ under pressure (Fig. 7). Most of the materials exhibit a decrease in ξ with pressure, in agreement with the results of recent simulations [50,51]. These simulations analyzed pressure dependence of the length scale L below which the homogeneous elastic continuum approximation for deformation breaks down and structural heterogeneity becomes important [50,51]. They found $L \propto P^{-x}$ with the exponent $x = 1/4$, which qualitatively agrees with the behavior of ξ observed for most of the materials (Fig. 7). Thus the general behavior for dynamic heterogeneities is a decrease of characteristic length scale under compression (densification).

However, two materials, OTP and glycerol, exhibit essentially no pressure-induced variations of ξ. This difference cannot be ascribed to intermolecular forces, since glycerol is a hydrogen bonding system, but OTP is a van der Waals bonding material, the same as cumene. It cannot be attributed to

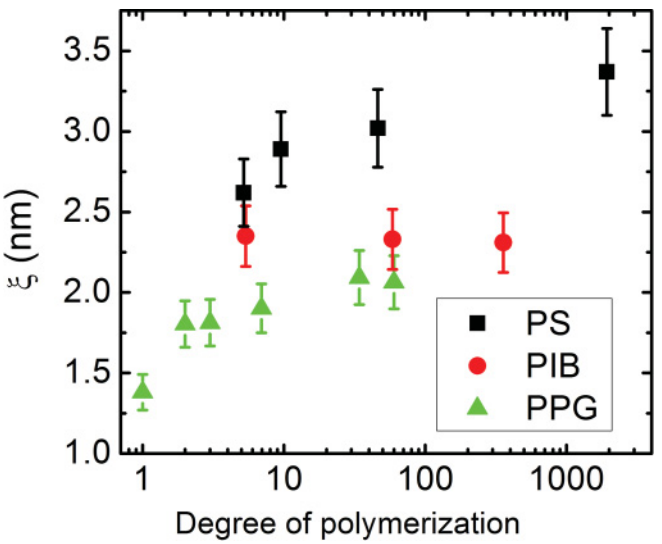

FIG. 3. (Color online) Dependence of ξ estimated from the boson peak on the degree of polymerization in PS, PIB, and PPG.

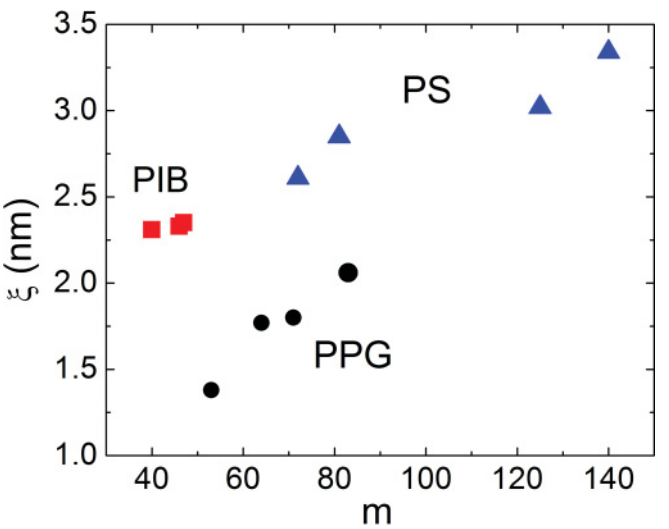

FIG. 4. (Color online) The heterogeneity length scale vs fragility for PS, PIB, and PPG of various molecular weights.

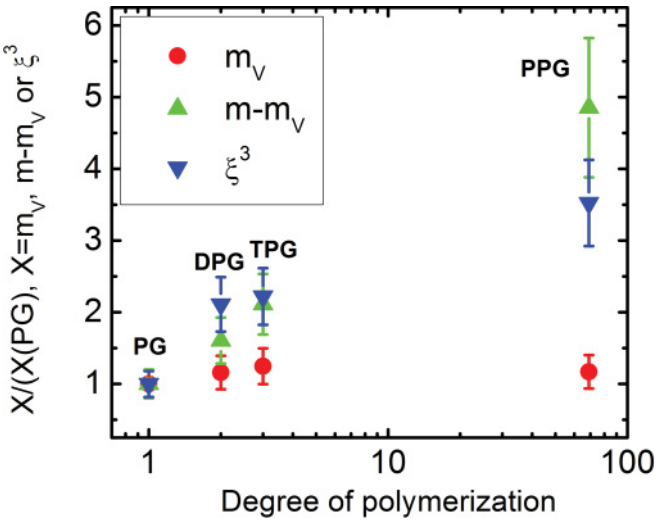

FIG. 5. (Color online) Dependence of the isochoric fragility, m_V, volume contribution to fragility, m–m_V, and heterogeneity volume ξ^3 on degree of polymerization in PPG. All the values are scaled by the value of the monomer (PG) ($m = 53$, $m_v = 47$, $\xi^3 = 2.63$ nm^3). Data for fragility are from [48,49].

the difference between polymers and small molecules, either. Cumene and short PS (MW $\approx$ 540) should be considered as small molecule systems, but exhibit the same behavior as polymers. Thus the reason for the particular behavior of ξ under pressure in these materials remains unknown.

As the next step we will compare the pressure-induced variations of the heterogeneity length scale and of the activation volume. It follows from Eq. (3) that $\Delta V^{\#} = k_B T \partial \ln \tau_\alpha / \partial P$. As at T_g one has $\ln \tau_\alpha$ = const by definition, one can obtain the expression connecting $\Delta V^{\#}$, dT_g/dP, and fragility m:

$$V^{\#}(T_g) = k_B m (dT_g/dP) \ln 10. \quad (5)$$

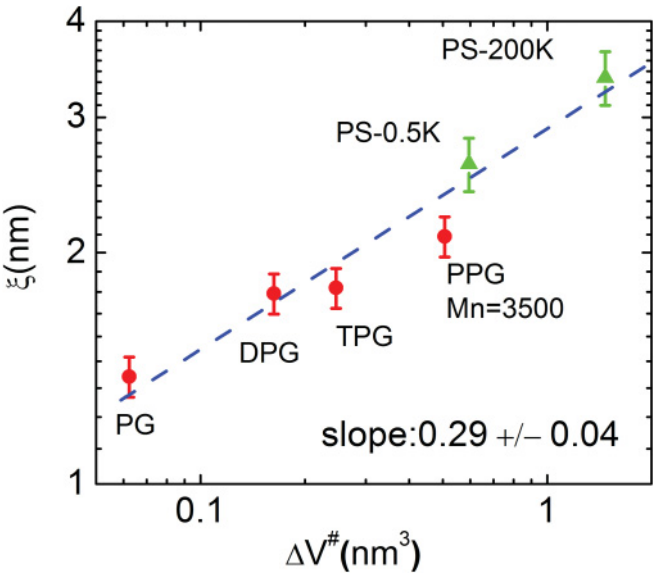

FIG. 6. (Color online) ξ vs $\Delta V^{\#}$ in PS (green triangles) and PPG (red circles) with different molecular weight. The dashed line is a linear fit of the data in a double-logarithmic plot.

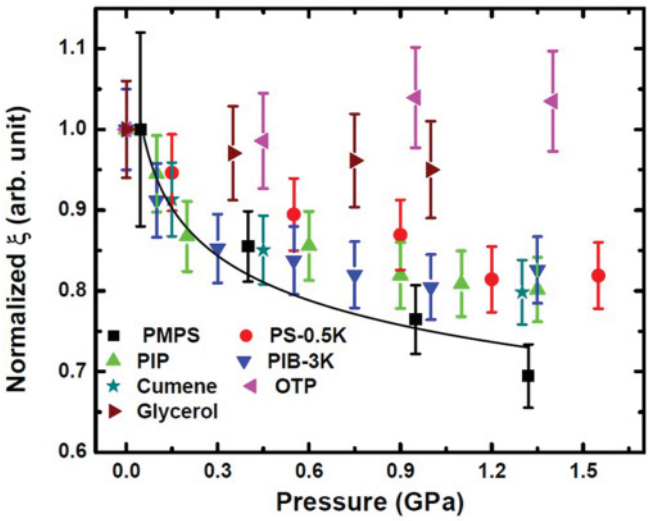

FIG. 7. (Color online) Pressure-induced variations of ξ in seven studied materials (data from [43]). The values of ξ are scaled by the values at ambient pressure. The solid line presents the dependence suggested from simulations [50].

According to Ref. [38], fragility should significantly decrease with pressure for most glass-forming materials. The value of dT_g/dP also drops with pressure, although the detailed pressure variation is material dependent [39,52]. As a product of m and dT_g/dP [Eq. (5)], $\Delta V^{\#}$ should reduce dramatically under densification in most glass-forming materials. This agrees with the observed pressure-induced decrease of ξ in most of the studied systems (Fig. 7). However, OTP and glycerol are exceptions: Fragility increases with increasing pressure in glycerol and remains constant in OTP (Table I). More specifically, as seen in Table I, fragility of glycerol increases by $\sim$20% from ambient pressure to 1 GPa, while dT_g/dP decreases by 23% [52]. Thus, the pressure-induced variations of the two parameters cancel one another. As a result, $\Delta V^{\#}$ is insensitive to pressure, in agreement with the behavior of ξ (Fig. 7). In the case of OTP, fragility remains constant up to 0.8 GPa [53], and dT_g/dP has only a slight decrease up to 0.1 GPa [54]. Although the experimental data of dT_g/dP at higher pressure are not available for OTP, we would not expect a strong pressure dependence of $\Delta V^{\#}$ in this material. We were able to find literature data for the pressure-induced variations of fragility and dT_g/dP for only four out of the seven systems presented in Fig. 7. Direct comparison of the

TABLE I. Parameters of the materials in the pressure study; x is the exponent from the fit $\xi \propto P^{-x}$ and all other parameters are from Refs. [36,38].

	T_g (K)	dT_g/dP (K/GPa)	m	dm/dP (GPa^{-1})	x
PMPS	247	280	100	0	0.10
PS-0.5K	253	260	72	–60	0.06
PIP	201	178	62	–40	0.06
PIB-3K	195	240	46		0.05
Cumene	126	86	93	–60	0.06
OTP	246	260	81	0	0.00
Glycerol	185	40	53	35	0.00

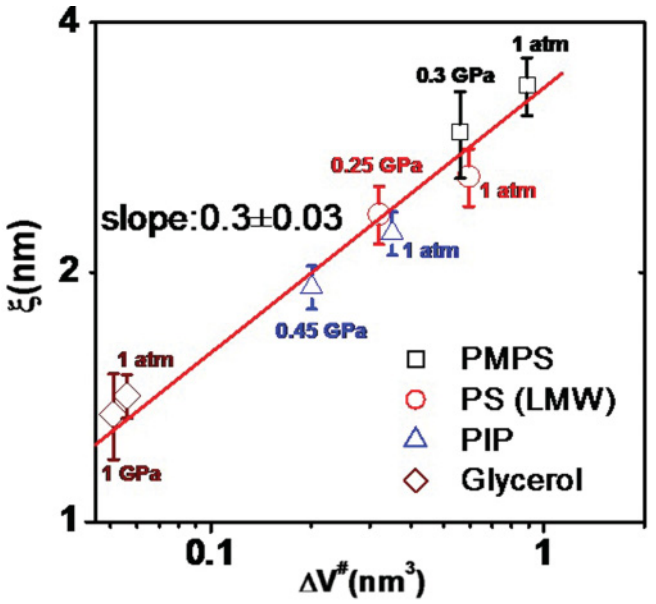

FIG. 8. (Color online) Correlation of ξ and $\Delta V^{\#}$ under pressure, the solid line presents a linear fit.

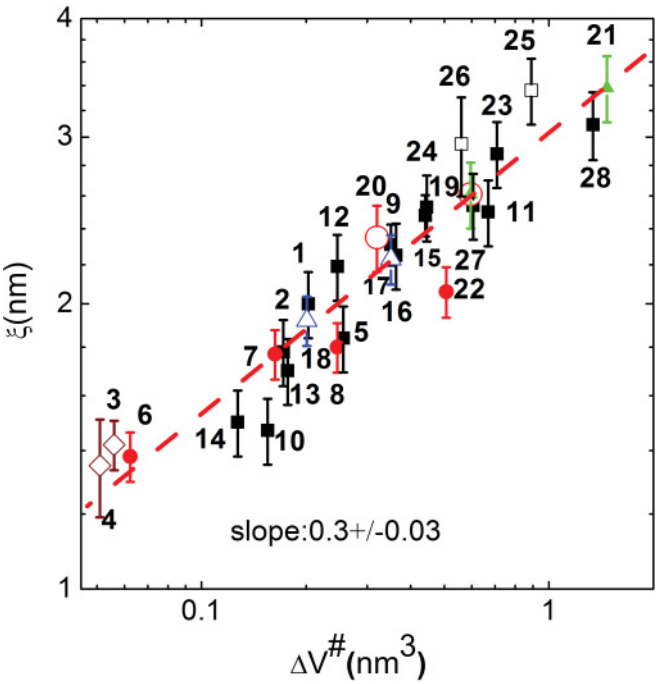

FIG. 9. (Color online) ξ vs $\Delta V^{\#}$ in a double-logarithmic scale, the linear fit (the dashed line) gives $\lg(\xi) = 0.48 + 0.3 \times \lg(\Delta V^{\#})$. Numbers represent the following glass-forming systems: (1) B_2O_3, (2) As_2S_3, (3) glycerol, (4) glycerol ($P = 1$ Gpa), (5) Se, (6) PG, (7) DPG, (8) TPG, (9) Salol, (10) DBP, (11) OTP, (12) Cumene, (13) CKN, (14) Sorbitol, (15) PIB (Mn = 20,000), (16) PnBMA, (17) PIP, (18) PIP (0.45 GPa), (19) PS ($M_n = 540$), (20) PS ($M_n = 540$, $P = 0.25$GPa), (21) PS ($M_n = 200{,}600$), (22) PPG, (23) PVAc, (24) PDMS, (25) PMPS, (26) PMPS ($P = 0.3$ GPa), (27) PMMA, and (28) PC. Solid squares: different systems at ambient condition; solid circles and triangles: molecular weight effect on ξ for PPG and PS, respectively; open squares, circles, triangles, and diamonds denote pressure dependence of ξ in PMPS, PS (LMW), PIP, and glycerol, respectively. The data on the materials in ambient conditions can be found in Refs. [36,37] and on the materials under pressure (see Table II).

pressure-induced variations for these four systems again reveals strong correlation between ξ and the activation volume (Fig. 8). The slope of the linear fit demonstrates that the proportional relationship between ξ^3 and $\Delta V^{\#}$ for these materials holds also under densification.

Figure 9 summarizes all the experimental data for ξ and $\Delta V^{\#}$ at T_g for chemically different materials, polymers with different molecular weights, and systems under pressure. We want to stress that there are no prefactors or corrections in all these data. Surprisingly, ξ estimated from the boson peak spectra always correlates with the activation volume estimated for the structural relaxation at T_g (Fig. 9). Moreover, the fit line suggests that on average $\Delta V^{\#} \approx 0.03\xi^3$ regardless of the chemical structure, the molecular weight, and the external pressure. It means that the sensitivity of the structural relaxation to density (pressure) is defined by the heterogeneity volume. In that respect hydrogen bonding systems have the lowest heterogeneity length scale among the materials studied here and that might explain their weak sensitivity of structural relaxation to pressure (small $\Delta V^{\#}$).

C. Temperature dependence of ξ

Up to this point we discussed the relation between fragility, activation volume, and the boson peak length scale ξ at one characteristic temperature, namely at T_g. With increasing T, the length of dynamical heterogeneity is expected to decrease. In this respect, it is interesting to investigate the temperature dependence of ξ above T_g. Figure 10 presents the temperature dependence of ξ in glycerol, OTP, PIB (all three are our measurements), and B_2O_3 (literature data from [55]). The length scale estimated from the boson peak does not exhibit any strong variations in the investigated temperature range for all studied materials. ξ does not depend on temperature within the experimental error bars for OTP (up to $1.08T_g$) and glycerol (up to $1.25T_g$). ξ slightly (~15%) rises in PIB

TABLE II. Data for materials under pressure presented in Fig. 9; m is fragility, c_t is the transverse sound velocity, ν_{bp} is the boson peak frequency, ξ is the boson peak length scale, $\Delta V^{\#}$ is the activation volume.

Systems	m	T_g (K)	dT_g/dP (K/GPa)	c_t (km/s)	ν_{bp} (GHz)	ξ (nm)	$\Delta V^{\#}$ (nm^3)
(4) Glycerol ($P = 1$ GPa)	60	223	27	2.35	1740	1.35	0.051
(18) PIP (0.45 GPa)	49	269	130	1.66	865	1.92	0.20
(20) PS-0.5K ($P = 0.25$ GPa)	55	306	190	1.41	600	2.35	0.32
(26) PMPS ($P = 0.3$ GPa)		320		1.4	465	3.08	0.56

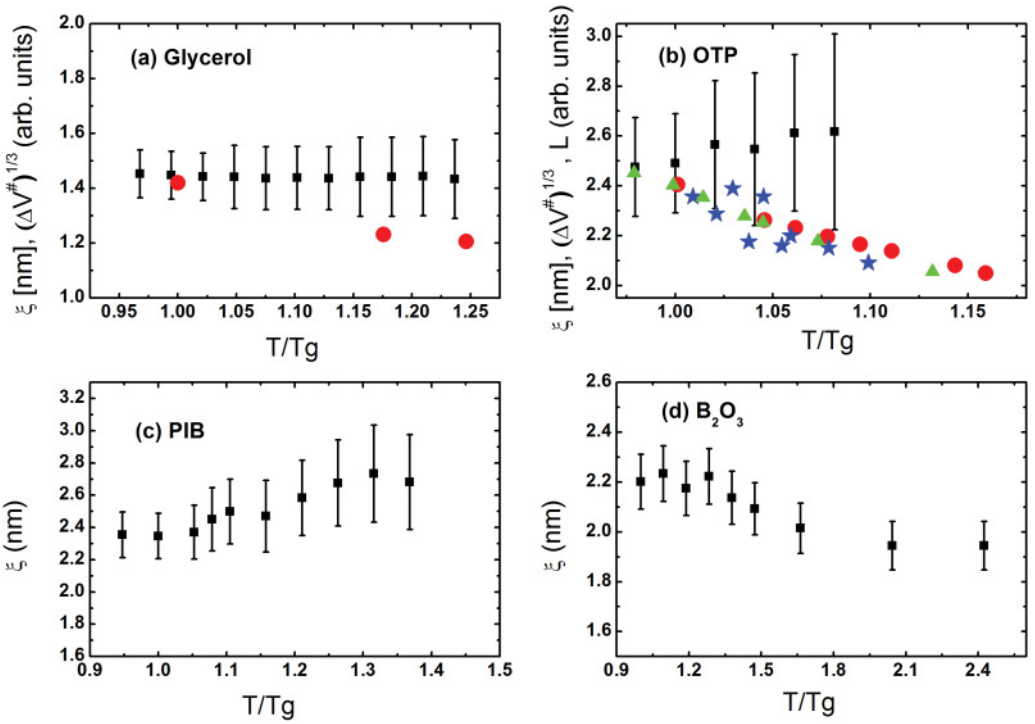

FIG. 10. (Color online) Temperature dependence of ξ (black squares) in (a) glycerol, (b) OTP, (c) PIB. Additionally data for B_2O_3 from [55] are shown in (d). Red circles: $(\Delta V^{\#})^{1/3}$ (scaled by an arbitrary prefactor) for glycerol (from [40]) and OTP (from [53]). (b) Stars: heterogeneity length from Ref. [56], triangles: cooperativity length from Ref. [59], both arbitrarily normalized.

between T_g and $1.3T_g$, and it slightly ($\sim$12%) decreases for B_2O_3 between T_g and $2T_g$. These results are surprising and contradict traditional model expectations. Unfortunately, there are only a few direct experimental measurements of the temperature dependence of dynamic heterogeneities length scale in glass-forming systems (we do not include the data obtained by the derivative analysis of χ_T for the reason discussed in the Introduction). We can compare our results for glycerol to the recent nonlinear dielectric studies [20] and earlier 4-D NMR measurements [24] (Fig. 11). Unfortunately, the error bars of the 4-D NMR measurements do not allow any quantitative conclusions. However, nonlinear dielectric measurements reveal a clear decrease in the number of dynamically correlated structural units $N_{\rm het}$ [20] with increase in temperature (Fig. 11): It decreases less than two times, which transfers to an expected decrease in heterogeneity length scale (assuming $L_{\rm het} \propto N_{\rm het}{}^{1/3}$) $\sim$20%–25%, clearly outside of our error bars. In Fig. 10(b) we also show the temperature dependence of the dynamic heterogeneity length in OTP that was estimated in Ref. [56] using a fluctuation model developed by Donth, and combined results of light scattering and viscosity experiments. These data agree surprisingly well with the temperature behavior of the activation volume in OTP [Fig. 10 (b)].

We note that the characteristic length for the glass transition was estimated in many publications on the basis of the Adam-Gibbs theory of cooperatively rearranging regions (CRR) [57]. The relation between the length scales of CRR and dynamical heterogeneity is not clear. At least, one can argue that the length of dynamical heterogeneities represents an upper limit for any cooperativity length [15,16], although one can think that these two length scales might be identical [16]. The number of particles in CRR as a function of temperature is determined, e.g., in Refs. [58–60] for some polymeric and low-weight molecular liquids. We emphasize that in this paper we concentrate on the dynamical heterogeneities, not on CRR. However, it is interesting to compare the temperature variations of the CRR size with $L_{\rm het}(T)$ and $\xi(T)$. Figure 10(b) presents the data of Ref. [59] for the temperature dependence of the size of CRR in OTP found on the basis of the Adam-Gibbs theory.

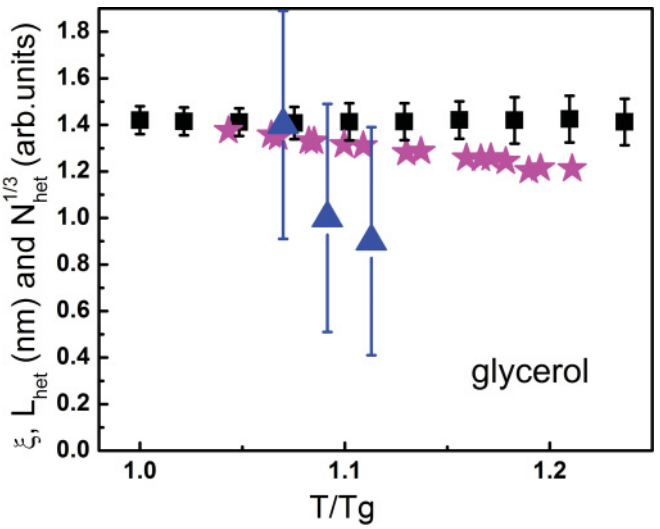

FIG. 11. (Color online) Temperature dependence of ξ in comparison with the dynamical heterogeneity length in glycerol. (Triangles: $L_{\rm het}$ from NMR measurements [24]; solid stars: $N_{\rm het}{}^{1/3}$ scaled by an arbitrary factor, where $N_{\rm het}$ is the number of molecules in dynamically correlated regions in glycerol from nonlinear dielectric measurements [20]).

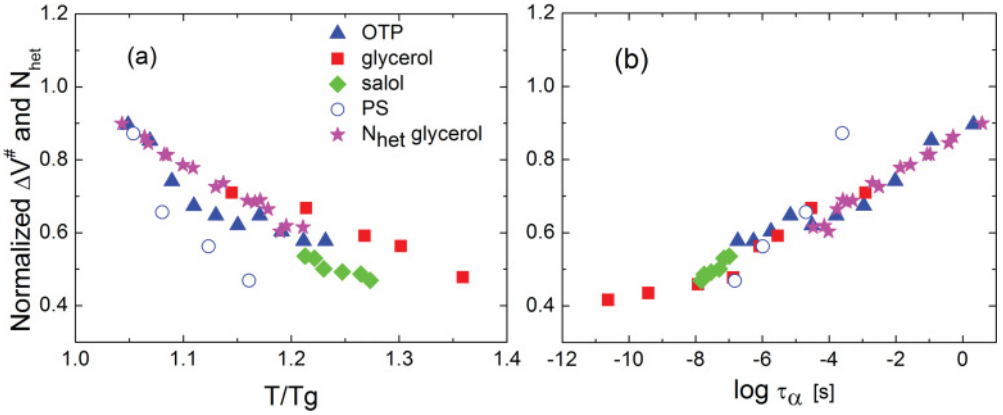

FIG. 12. (Color online) (a). T dependence of the activation volume in various systems (solid squares: glycerol; diamonds: salol; triangles: OTP; circles: PS) in comparison with the number of molecules in dynamically correlated regions in glycerol from nonlinear dielectric measurements $N_{\rm het}$ [20] (stars).The amplitudes of the data are scaled by an arbitrary factor to make a master curve. (b) The same data as a function of the α-relaxation time τ_α. The data for $\tau_\alpha(T)$ are from Refs. [61] (glycerol), [62] (OTP), [63] (salol), and [64] (PS).

It agrees well with the data of Fischer *et al*. [56] and with the temperature dependence of the activation volume $\Delta V^{\#}(T)$.

Also important is the difference in temperature behavior of $\xi(T)$ and $\Delta V^{\#}(T)$ [Figs. 10(a) and 10(b)]. It is known that all materials usually exhibit a decrease in the activation volume with temperature [39–42]. Analysis of the data for glycerol actually show that $N_{\rm het}(T)$ and $\Delta V^{\#}(T)$ have very similar temperature variations (Fig. 12). Temperature variations of $V^{\#}(T)$ in OTP also appear to be similar to $L_{\rm het}(T)$ estimated by Fisher *et al*. [Fig. 10(b)]. These observations support our earlier conclusion that there might be a strong connection between the heterogeneity volume and activation volume. It is interesting to note that $\Delta V^{\#}$ has very similar temperature dependence in various materials [except the lowest temperature point for PS; see Fig. 12(a)]. This similarity is even better if the activation volume is plotted vs the α-relaxation time [Fig. 12(b)]. This means that the relative change of $\Delta V^{\#}$ with temperature might be determined entirely by the value of τ_α.

Thus the observed temperature dependence of $\xi(T)$ is contradictory to the expected decrease in dynamic heterogeneity length scale (that has been confirmed experimentally [20,24]) and to the known behavior of $\Delta V^{\#}(T)$ (Figs. 10–12). This is a puzzling observation and suggests that the assumption connecting $c_t/\nu_{\rm bp}$ to $L_{\rm het}$ is incorrect. So far, we do not have a clear explanation for this result. First of all, the expected decrease in $\xi(T)$ in the studied temperature range is not very high, maybe ~20%–30% (Figs. 10 and 11). But this is obviously outside the error bars of our measurements. One should note that the temperature dependence of the ratio $c_t/\nu_{\rm bp}$ does not exactly correspond to that of the length scale ξ because the prefactor S in Eq. (1) might vary with temperature. As predicted by the elastic constant fluctuation model, increasing the amplitude of the elastic constant's fluctuations would decrease S (Fig. 1 of Ref. [33]), i.e., at a fixed correlation radius the wavelength of the quasilocalized vibration $c_t/\nu_{\rm bp}$ will decrease with increasing amplitude of fluctuation. This follows also from a simple model of Ref. [65] in which the mean free path L of an acoustic vibration is estimated as Rayleigh scattering due to static fluctuations of elastic properties with a correlation length ξ. Assuming that at the boson peak frequency the Ioffe-Regel criterion of localization for transverse waves is fulfilled, they obtained

$$\xi \propto (\langle \Delta c^2/c^2\rangle)^{-1/3} c/\nu_{\rm bp}. \tag{6}$$

Qualitatively this relation confirms that the factor $S \propto 1/\langle(\Delta c/c)^2\rangle^{1/3}$ decreases with increasing fluctuation amplitude. In general, lowering the temperature of equilibrium liquid would reduce the amplitude of fluctuations. As a result, S will increase with cooling and decrease with heating. This means that even if $c_t/\nu_{\rm bp}$ does not change much with T, actually ξ may increase with decreasing temperature. The overall variations of S might be ~20%–30% (Figs. 10–12). The existing data do not allow us the possibility of making a quantitative estimation of $S(T)$, and only qualitative conclusion is available at the moment. However, T dependence of the factor S may, in principle, explain the difference in temperature dependence of $c_t/\nu_{\rm bp}$ and $L_{\rm het}$.

At this point we want to comment additionally on a good correlation between variations of ξ and $\Delta V^{\#}$ under pressure (Sec. III B and Figs. 8 and 9). It is usually expected that change in pressure might have similar effects as changes in temperature. However, our analysis of variations of ξ and $\Delta V^{\#}$ under pressure has been done at T_g. It means that the increase in pressure was compensated for by an increase in the glass transition temperature $T_g(P)$. As a result the change in amplitude of fluctuations at $T_g(P)$ and corresponding change in the parameter S were not significant, in contrast to the temperature variations above T_g analyzed here.

IV. CONCLUSIONS

We studied the correlation between the heterogeneity length scale estimated from the boson peak and activation volume in various molecular, hydrogen-bonding, and polymeric glass formers. Regardless of change in chemical structure, molecular weight, and pressure (density) of the studied materials the same correlations $\xi^3(T_g) \propto \Delta V^{\#}(T_g)$ have been observed. This is valid even for glycerol and OTP, where the pressure

dependence of both parameters is very weak. We showed also that the number of dynamically correlated particles in glycerol as a function of temperature is proportional to the activation volume. These results support the idea that sensitivity of structural relaxation to density (the activation volume) might be connected to the length scale of dynamic heterogeneity in the material. However, analysis of the temperature variations of $\xi(T)$ above T_g provides a puzzling result: There are no significant changes of the ratio $c_t(T)/\nu_{\rm bp}(T)$ for studied materials, while the activation volume and the heterogeneity length scale estimated using other experimental technique clearly decrease with temperature above T_g. We argue that the prefactor S that connects the heterogeneity length scale ξ to the wavelength of the boson peak vibration $c_t/\nu_{\rm bp}$ might decrease with increasing temperature that masks the temperature dependence of $\xi(T)$. This point requires further investigation.

ACKNOWLEDGMENTS

A.P.S. acknowledges the support from the Division of Materials Sciences and Engineering, DOE Office of Basic Energy Sciences. V.N.N acknowledges the financial support from the LDRD Program of ORNL, managed by UT-Battelle, LLC, LOIS#: 5843, for DOE, and from the RFBR (Grant No. 09-02-01297a).

[1] M. D. Ediger, Annu. Rev. Phys. Chem. **51**, 99 (2000).
[2] R. Richert, J. Phys. Condens. Matter **14,** R703 (2002).
[3] S. C. Glotzer, J. Non-Cryst. Solids **274**, 342 (2000).
[4] *Dynamical Heterogeneities in Glasses, Colloids and Granular Materials,* edited by L. Berthier, G. Biroli, J.-P. Bouchaud, L. Cipelletti, and W. van Saarloos, International Series of Monographs on Physics, Vol. 150 (Oxford University Press, Oxford, 2011).
[5] A. Widmer-Cooper and P. Harrowell, Phys. Rev. Lett. **96**, 185701 (2006).
[6] E. R. Weeks, J. C. Crocker, A. C. Levitt, A. Schofield, and D. A. Weitz, Science **287**, 627 (2000).
[7] C. Donati, S. Franz, S. C. Glotzer, and G. Parisi, J. Non-Cryst. Solids **307**, 215 (2002).
[8] S. Glotzer, V. Novikov, and T. Schrøder, J. Chem. Phys. **112**, 509 (2000).
[9] L. Berthier, G. Biroli, J.-P. Bouchaud, and R. L. Jack, in *Dynamical Heterogeneities in Glasses, Colloids, and Granular Media*, edited by L. Berthier, G. Biroli, J.-P. Bouchaud, L. Cipelletti, and W. van Saarloos (Oxford University Press, New York, 2011), Chap. 3.
[10] R. Candelier, A. Widmer-Cooper, J. K. Kummerfeld, O. Dauchot, G. Biroli, P. Harrowell, and D. R. Reichman, Phys. Rev. Lett. **105**, 135702 (2010).
[11] C. Donati, S. C. Glotzer, P. H. Poole, W. Kob, and S. J. Plimpton, Phys. Rev. E **60**, 3107 (1999).
[12] A. Duri and L. Cipelletti, Europhys. Lett. **76**, 972 (2006).
[13] I. S. Aranson and L. S. Tsimring, Rev. Mod. Phys. **78**, 641 (2006).
[14] A. Ferguson and B. Chakraborty, Europhys. Lett. **78**, 28003 (2007).
[15] U. Tracht, M. Wilhelm, A. Heuer, H. Feng, K. Schmidt-Rohr, and H. W. Spiess, Phys. Rev. Lett. **81**, 2727 (1998).
[16] X. H. Qiu and M. D. Ediger, J. Phys. Chem. B **107**, 459 (2003).
[17] C. Dalle-Ferrier, C. Thibierge, C. Alba-Simionesco, L. Berthier, G. Biroli, J.-P. Bouchaud, F. Ladieu, D. L'Hôte, and G. Tarjus, Phys. Rev. E **76**, 041510 (2007).
[18] J.-P. Bouchaud and G. Biroli, Phys. Rev. B **72**, 064204 (2005).
[19] M. Tarzia, G. Biroli, A. Lefevre, and J.-P. Bouchaud, J. Chem. Phys. **132**, 054501 (2010).
[20] C. Crauste-Thibierge, C. Brun, F. Ladieu, D. L'Hôte, G. Biroli, and J.-P. Bouchaud, Phys. Rev. Lett. **104**, 165703 (2010).
[21] K. Vollmayr-Lee, W. Kob, K. Binder, and A. Zippelius, J. Chem. Phys. **116**, 5158 (2002).
[22] A. P. Sokolov and K. S. Schweizer, Phys. Rev. Lett. **102**, 248301 (2009).
[23] C. Dasgupta, A. V. Indrani, S. Ramaswamy, and M. K. Phani, Europhys. Lett. **15**, 307 (1991).
[24] S. A. Reinsberg, X. H. Qiu, M. Wilhelm, H. W. Spiess, M. D. Ediger, J. Chem. Phys. **114**, 7299 (2001).
[25]]. L. Berthier, G. Biroli, J.-P. Bouchaud, L. Cipelletti, D. El Masri, D. L'Hote, F. Ladieu, and M. Pierno, Science **310**, 1797 (2005).
[26] D. J. Ashton and J. P. Garrahan, Eur. Phys. J. E: Soft Matter Biol. Phys. **30**, 303 (2009).
[27] J. Dudowicz, K. F. Freed, and J. F. Douglas, J. Phys. Chem. B **109**, 21350 (2005).
[28] V. K. Malinovsky and A. P. Sokolov, Solid State Commun. **57**, 757 (1986).
[29] V. K. Malinovsky, V. N. Novikov, and A. P. Sokolov, Chem. Phys. Lett. **143**, 111 (1988).
[30] E. Duval, A. Boukenter, and T. Achibat, J. Phys. Condens. Matter, 10227 (1990).
[31] J. Jäckle, in *Amorphous Solids: Low-Temperature Properties*, edited by W. A. Phillips (Springer, Berlin, 1981).
[32] E. Courtens, M. Foret, B. Hehlen, and R. Vacher, Solid State Commun. **117**, 187 (2001).
[33] W. Schirmacher, B. Schmid, C. Tomaras, G. Viliani, G. Baldi, G. Ruocco, and T. Scopigno, Phys. Status Solidi C **5**, 862 (2008).
[34] V. Lubchenko and P. G. Wolynes, Annu. Rev. Phys. Chem. **58**, 235 (2007).
[35] P. G. de Gennes, C. R. Phys. **3**, 1263 (2002).
[36] L. Hong, P. D. Gujrati, V. N. Novikov, and A. P. Sokolov, J. Chem. Phys. **131**, 194511 (2009).
[37] L. Hong, V. N. Novikov, and A. P. Sokolov, J. Non-Cryst. Solids **357**, 351 (2011).
[38] C. M. Roland, S. Hensel-Bielowka, M. Paluch, and R. Casalini, Rep. Prog. Phys. **68**, 1405 (2005).
[39] G. Fytas, T. Dorfmuller, and C. H. Wang, J. Phys. Chem. **87**, 5041 (1983).
[40] G. P. Johari and E. Whalley, Faraday Symp. Chem. Soc. **3**, 23 (1972).
[41] G. D. Patterson, P. J. Carroll, and J. R. Stevens, J. Polym. Sci., Polym. Chem. Ed. **21**, 605 (1983).

[42] R. Casalini, M. Paluch, and C. M. Roland, J. Phys. Chem. A **107**, 2369 (2003).
[43] L. Hong, B. Begen, A. Kisliuk, C. Alba-Simionesco, V. N. Novikov, and A. P. Sokolov, Phys. Rev. B **78**, 134201 (2008).
[44] C. H. Whitfield, E. M. Brody, and W. A. Bassett, Rev. Sci. Instrum. **47**, 942 (1976).
[45] A. Jayaraman, Rev. Sci. Instrum. **57**, 1013 (1986).
[46] A. P. Sokolov, N. V. Novikov, and Y. F. Ding, J. Phys. Condens. Matter **19**, 205116 (2007).
[47] K. Kunal, M. Paluch, C. M. Roland, J. E. Puskas, Y. Chen, and A. P. Sokolov, J. Polym. Sci. B **46**, 1390 (2008).
[48] C. Leon, K. L. Ngai, and C. M. Roland, J. Chem. Phys. **110**, 11585 (1999).
[49] R. Casalini and C. M. Roland, J. Chem. Phys. **119**, 11951 (2003).
[50] M. Wyart, L. E. Silbert, S. R. Nagel, and T. A. Witten, Phys. Rev. E **72**, 051306 (2005).
[51] L. E. Silbert, A. J. Liu, and S. R. Nagel, Phys. Rev. Lett. **95**, 098301 (2005).
[52] M. Paluch, R. Casalini, S. Hensel-Bielowka, and C. M. Roland, J. Chem. Phys. **116**, 9839 (2002).
[53] K. U. Schug, H. E. King, and R. Bohmer, J. Chem. Phys. **109**, 1472 (1998).
[54] T. Atake and C. A. Angell, J. Phys. Chem. **83**, 3218 (1979).
[55] L. Börjesson, A. K. Hassan, J. Swenson, L. M. Torell, and A. Fontana, Phys. Rev. Lett. **70**, 1275 (1993).
[56] E. W. Fischer, E. Donth, and W. Steffen, Phys. Rev. Lett. **68**, 2344 (1992).
[57] G. Adam and J. H. Gibbs, J. Chem. Phys. **43**, 139 (1965).
[58] D. Cangialosi, A. Alegría, and J. Colmenero, Phys. Rev. E **76**, 011514 (2007).
[59] O. Yamamuro, I. Tsukushi, A. Lindqvist, S. Takahara, M. Ishikawa, and T. Matsuo, J. Phys. Chem. B **102**, 1605 (1998).
[60] A. Saiter, L. Delbreilh, H. Couderc, K. Arabeche, A. Schönhals, and J.-M. Saiter, Phys. Rev. E **81**, 041805 (2010).
[61] P. Lunkenheimer, U. Schneider, R. Brand, and A. Loidl, Contemp. Phys. **41**, 15 (2000).
[62] C. Hansen, F. Stickel, T. Berger, R. Richert, and E. W. Fischer, J. Chem. Phys. **107**, 1086 (1997).
[63] F. Stickel, E. W. Fischer and R. Richert, J. Chem. Phys. **102**, 6251 (1995).
[64] Y. He, T. R. Lutz, M. D. Ediger, C. Ayyagari, D. Bedrov, G. D. Smith, Macromolecules **37**, 5032 (2004).
[65] D. Quitmann, M. Soltwisch, G. Ruocco, J. Non-Cryst. Solids **203**, 12 (1996).